Pressure Dependence of Near-Field Plume Properties in a 1kW Laboratory Hall Thruster

IEPC-2017-20

Presented at the 35th International Electric Propulsion Conference
Georgia Institute of Technology • Atlanta, Georgia • USA
October 8 – 12, 2017

Taylor S. Matlock[1] and Michael R. Nakles[2] and Rostislav Spektor[3]
The Aerospace Corporation, El Segundo, CA, 90245, USA

Abstract: The impact of facility background pressure on the near field plasma and neutral flow properties of a 1kW Hall thruster are examined using a planar Langmuir probe and a screened ionization gauge. An in situ calibration of the ionization gauge-based neutral flux probe is attempted using the ion flux of the Hall thruster beam as a known flow of xenon atoms. Experiments using a pair of neutral flux probes suggest a systematic error in the probing method. Near field Langmuir probe measurements show a global decrease in the electric field strength as the background pressure is increased several decades. A 4-8 MHz fluctuation is observed in the anode current and cathode-to-ground voltage that exhibits a linear increase in frequency with background pressure. The implications of these observations on mechanisms for Hall thruster dependence on background neutrals are discussed.

Nomenclature

β	=	pressure change normalized by transmission, ion flux and a constant, $\Delta P/T_1\Gamma_i S$
ΔP	=	pressure change from ion passing to ion retarding, $P(f=1)-P(f=0)$, Pa
f	=	fraction of ions with axial energy greater than the ion retarding voltage
Γ_i	=	flux of xenon ions, m^{-2}s^{-1}
Γ_n	=	flux of xenon neutrals, m^{-2}s^{-1}
M	=	xenon mass, kg
n_e	=	electron density, , m^{-3}
P_{gauge}	=	pressure measured by ionization gauge, Pa
S	=	wall temperature dependent constant, $\sqrt{2\pi M T_{gauge}}$
T_1	=	transmission fraction of first mesh
T_{gauge}	=	wall temperature of ionization gauge assembly, K

I.Introduction

ELECTRIC propulsion test facilities allow a reflux of propellant to reach the device under test due to a finite ability to pump particles that reach vacuum chamber surfaces. The reflux of particles has been shown to alter operational characteristics of Hall thrusters such as performance, erosion rates, oscillations and various plasma properties[1-6]. An early analysis of the effect of facility neutrals on Hall thrusters considered the rate of ingestion of neutrals by the thruster channel as the main metric[7], however most studies show ingestion estimates significantly underestimate the change in anode flow required to maintain a constant anode current. Nevertheless, a recent study suggests that neutral ingestion is grossly underestimated by the assumption that the flux of neutrals towards the thruster corresponds to a

[1] Member of the Technical Staff, Propulsion Science Department, taylor.matlock@aero.org.
[2] Propulsion Test Engineer, Propulsion Science Department, michael.nakles@aero.org.

thermal flux at the measured pressure, and indeed may be the dominant mechanism for the observed changes in operation[8].

Here we add another investigation of background pressure interactions with a Hall thruster with specific care towards validating our measurements of backstreaming neutral flux. Prior pressure effect studies at The Aerospace Corporation utilized an internal ionization gauge mounted on a 'tee'[2-4], which from a simple analysis (recreated below) should measure the pressure at which the thermal flux is equal to the non-thermal flux of neutrals entering the probe, and so should not result in the discrepancies described Ref. 8 where they are applied to Ref.4. We attempt validating this technique by altering the pressure probe operation to measure the flux of ions from the Hall thruster plume and comparing the result to planar Langmuir probe measurements. The uncertainty remains high for this initial test, but some paths for improvement are described.

In addition, we use a miniature planar Langmuir probe to map the plasma parameters in the near field of the thruster. These measurements suggest a decreasing electric field strength and increased ion beam collimation in the near field as the background pressure is raised. The resulting maps, though obscured by the intrusive nature of the measurement, can be used to validate the models that will ultimately be necessary to determine how to extrapolate from operation in a terrestrial vacuum chamber to on-orbit characteristics. Of particular interest is a decrease in the electric field strength throughout the near-field as pressure is increased which has implications for electron confinement and beam neutralization.

A discussion of the changes in observed thruster fluctuations with pressure is also presented with a focus on frequencies near the ion plasma frequency in the near field plume (~5 MHz). A variety of studies have shown the impact of background pressure on the ubiquitous breathing mode found in Hall thrusters in the 10-50 kHz frequency range, but little information is available in the open literature on the effects of finite facility pumping on higher frequency fluctuations in the 1-10 MHz range, where much of the recent work concerning electron transport has focused. We report on a particularly pressure sensitive mode in the 4-8 MHz range.

II.Experimental Apparatus

Experiments were performed using a nominally 1kW laboratory Hall thruster from the Princeton Plasma Physics Laboratory[2,9]. For the following tests the thruster is run at a constant voltage (300 V) and power (500 W) with a constant cathode flow rate (2.2 sccm of xenon) and matched outer and inner magnet settings (1.5 A each for an expected peak field strength near 100 G). The anode flow rate is adjusted manually during testing to ensure the discharge current remains constant and ranged between 18.7 and 19.6 sccm of xenon across a 25-fold increase in background pressure.

The discharge power supply was equipped with an LC filter with a 125μH inductor between the high side of the power supply and a 23μF capacitor. The other side of the capacitor connects to the low side of the power supply output. The Heatwave cathode is oriented in the 12 o'clock position roughly 1.125" downstream of the outer pole at a radius of 2.75" and declination of 50° (from thruster axis). The inner magnetic pole is covered by a 1/8" thick ceramic cap, while the outer pole is an exposed conducting surface.

Two separate experiments were performed with the same thruster and facility, but with a different configuration of neutral flux probe (see next section). For the first configuration, with what is called the 'heritage' probe, the thruster body was grounded through the propellant lines. For the second configuration, with the 'apertured' probe, , the thruster body was grounded by wire external to the chamber so that the current could be measured, the anode power supply was swapped for a lower power model, and a stationary emissive probe was placed in the near field of the thruster plume.

Anode current is monitored with a Tektronix TCP303 current probe and TCPA300 amplifier with a -3dB bandwidth of 15 MHz on a 12-bit TDS 3014B oscilloscope. The cathode-to-ground voltage is measured directly on the o-scope and the thruster body current (measured only during the apertured probe experiment) is measured with a Tektronix TCP202A current probe with >50MHz bandwidth).

The thruster was operated in a 2.4-m diameter × 9.8-m long cryopumped vacuum chamber called EP2. Two reentrant cryopumps were on the end dome behind the thruster, four more reentrant pumps were in the beam dump region, and four 1.3-m cryotubs were mounted on the cylindrical wall of the chamber adjacent to the thruster. One of the 1.3-m cryotubs (at 9 o'clock and upstream of the thruster) was not operational during the 'heritage' probe tests. The base pressure with no gas load and 9 pumps running was approximately 3×10^{-7} Torr N_2 for the majority of testing. Background pressure was measured with a Stabil-Ion gauge located on the tank wall adjacent to the thruster. Working pressure measurements reported in this document have been corrected using the scale factor of 0.348 specified by the gauge manufacturer for xenon relative to nitrogen. Facility effects were investigated at the 300V/500W condition by using auxiliary xenon flow introduced near the axial midpoint of the chamber.

A. Xenon Flux Measurement

Neutral xenon flux backstreaming towards the thruster channel is an important metric in characterizing the effect of the finite facility pumping on thruster operation. Prior testing at The Aerospace Corporation has utilized an accommodation volume approach to measuring neutral flux where a 2-¾ inch conflat 'tee' is placed adjacent to the thruster with one tube end placed to accept the backstreaming neutral flux, the opposite tube end is closed with a blank flange, and the tube end at 90° is fitted with a Granville Phillips Stabil-ion gauge[3]. A pair of wire meshes at the inlet can be used to repel electrons and ions. In this configuration the incoming neutral xenon flux thermalizes with the walls of the 'tee' (the accommodation volume) before reaching the ionization gauge. At steady-state the flux of particles into the 'tee' equals the approximately thermal flux of xenon neutrals out and so the pressure measurement of the ionization gauge can be used as a direct measurement of the neutral flux using Eq. (1). This principle was used by King and Gallimore to make a similar gridded neutral flux probe for Hall thruster plume studies, though without the 90° section[10].

$$\Gamma_n = \frac{P_{gauge}}{\sqrt{2\pi M T_{gauge}}} \tag{1}$$

Equation (1) assumes complete accommodation of the incoming flux with the walls of the 'tee' at temperature T_{gauge}, which is expected to be accurate due to the multiple wall collisions necessary for inflowing neutrals to reach the ionization gauge volume.

Another key assumption in the application of Eq. (1) is that the fraction of the inward-going neutral flux impinging on the inlet area that will make it to the ionization gauge volume is equal, or roughly equal, to the fraction of the outward-going neutral flux from the ionization gauge volume that makes it out of the neutral flux probe assembly. Said another way, the effective Clausing factor between particles entering the probe and entering the ionization gauge volume is the same in either direction. This assumption is not valid, for example, for ions that are electrostatically repelled by the ion retarding grid, because now the probability that an initially ionized xenon particle will reach the ionization gauge is not the same as the probability that a neutral from the ionization gauge will exit the probe. Another example of effective Clausing factor asymmetry is the case of different grid transmission probabilities for an ion beam compared to thermal neutrals.

The simplest scenario is for a probe that electrostatically repels ions with a single grid, allowing only a fraction *f* to pass the potential barrier. In this case the pressure in the gauge is related to the 1-sided ion flux entering the probe, Γ_i, by the relation, $P_{gauge} = f\Gamma_i S$, where $S = \sqrt{2\pi M T_{gauge}}$, which differs from Eq. (1) only by the factor *f*.

The relation between gauge pressure and 1-sided ion flux for a multi-grid system becomes more complicated. For example, our heritage neutral flux probe has an inlet grid biased to repel electrons (a small electron flux to the ionization gauge can cause large spurious readings) upstream of the ion retarding grid. In this case, electrostatically reflected ions that impinge on the electron repelling mesh are neutralized and the flux of recombined neutrals off the mesh then contribute to the neutral flux into the probe. This can be captured in the simplest case by Eq. (2), where we consider a single grid of transparency, T_1, in between the ion retarding grid and the probe inlet/outlet. The ion retarding potential electrostatically allows a fraction *f* of the incident ions to pass.

$$\Gamma_i = \frac{P_{gauge}}{[1 - T_1(1-f)]S} \tag{2}$$

Equation (2) gives the flux of ions entering the gauge based on the measured pressure, P_{gauge}, assuming the ions constitute the only incident particle flux. This equation is based on a simple geometric analysis and shows that when all ions are able to pass the ion retarding grid potential (f=1) the pressure measured by gauge represents the entire incident flux, but when all ions are reflected by the ion grid potential (f=0) the measured pressure corresponds to the flux of neutrals from recombination of ions at the electron repelling grid. When there are both neutral and ion fluxes entering the probe the pressures in Eqs. (1) & (2) can be added together (assuming no interaction between the ion and neutral fluxes in the probe) to yield Eq. (3).

$$P_{gauge} = S(\Gamma_n + \Gamma_i[1 - T_1(1-f)]) \tag{3}$$

The difference in the pressure measured by the gauge when *f*=1 and *f*=0 corresponds to the reflected ion flux that is transmitted through the electron repelling grid when *f*=0, as shown in Eq. 4. According to this simple theory, the accuracy of the neutral flux gauge can be validated against a known ion flux by measuring ΔP. If the theory and measurements are accurate we expect to find $\beta \equiv \Delta P/(ST_1\Gamma_i) = 1$.

$$\Delta P = P_{gauge}(f = 1) - P_{gauge}(f = 0) = ST_1\Gamma_i \quad (4)$$

The experiments described here utilize two configurations of the neutral flux probe with slightly different designs. The first is the heritage probe used by Diamant et al which has a 1-3/8 inch inlet diameter and two meshes with approximately 38% optical transparencies. The second design, which is referred to here as the aperture probe, has a small inlet aperture (1/4 inch diameter) in a stainless steel front plate with a coarse electron repelling mesh ($T_1 = 0.65$) attached (i.e. the entire front aperture plate is biased to repel electrons). The electron repelling grid is separated by a 0.008 inch thick Mica sheet from a 2-3/4 inch rotatable conflat flange which entrains the ion retarding electrode ($T_2 = 0.65$) so that the ion grid is approximately 0.3 inches from the electron grid. Both configurations are shown schematically in Fig. 1.

The ionization gauge and controller used in the experiments described here were calibrated with nitrogen using a NIST standard spinning rotor gauge. A linear least squares calibration fit gives a maximum extrapolation error of 4.4×10^{-7} Torr (N_2) over the range of pressures measured in these experiments. We add an additional uncertainty of 10% to all pressure measurements in quadrature with the extrapolation error before applying a xenon correction factor of 0.348. The added 10% uncertainty is intended to reflect some of the additional sources of uncertainty such as error in the xenon correction factor.

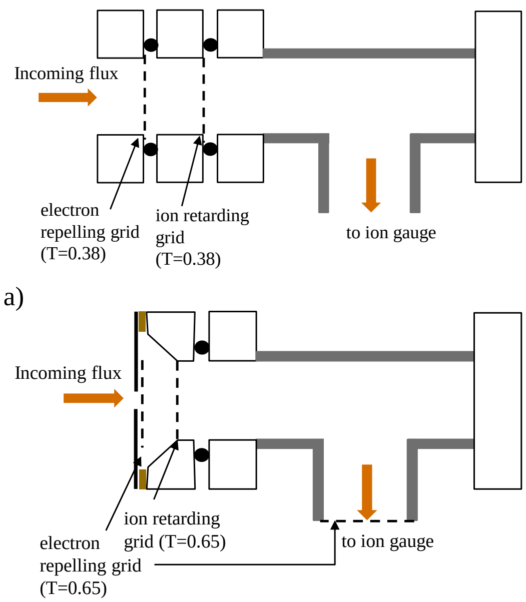

Figure 1. Neutral flux probe diagram for a) the heritage probe and b) the apertured probe

B. Near Field Langmuir Probe

A near-field (1-10 cm axially from exit) Langmuir probe is of the planar design, consisting of a 1-mm diameter tungsten wire (polished on the plasma facing side) set flush with a ¼” diameter boron nitride cap. The cap connects the probe to a 1/8” diameter alumina tube (6” long) which insulates the probe leads before dog-legging to a 24” long run of ¼” diameter alumina tubing. The signal is routed through shielded twisted pair cabling with the paired conductor connected to the high side of the probe biasing power supply (Kepco BOP 100-1M).

The near field probe current is measured across a shunt resistor (1.3 Ohms) with one side of the shunt going straight to the probe lead and the other to the high side of the bias supply. The voltage across the shunt is set as the input to an isolation amplifier (Avago ACPL-790B) the output of which goes to an NI USB-6363 DAQ. The bias supply is driven by a function generator set to provide a triangular waveform at 200 Hz and 1 V amplitude. The output voltage is also measured by the DAQ through a 10:1 voltage divider (10 kΩ impedance to ground). Probe current and voltage are measured by the multiplexed DAQ at a sampling rate of 250kHz, which is near the 3dB bandwidth of the isolation-amplifier. An RC filter is used on the input side of the isolation amplifier with a design 3-dB frequency of 250kHz to prevent aliasing and electrolytic capacitors are used on the power supply inputs to the isolation amplifier to decouple power supply noise from the circuit.

III.Results & Discussion

Two separate experiments were run with the same 1-kW Hall thruster operating at 300V and 1.67A at the anode. The first experiment used the heritage xenon flux probe while the second employed the apertured probe. The thruster telemetry, such as anode flow rate and cathode-to-ground potential were not identical between the two tests but showed some similar trends as shown in Fig. 2. The error bars in Fig. 2b) represent the standard deviation in fluctuations measured averaged over multiple waveforms each captured with 0.1μs resolution in 1ms long clips and do not represent uncertainty in the time-averaged values plotted.

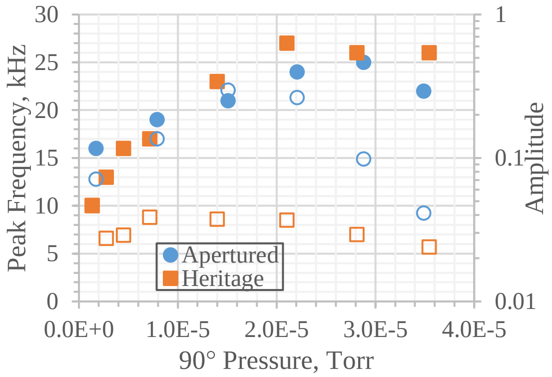

a)

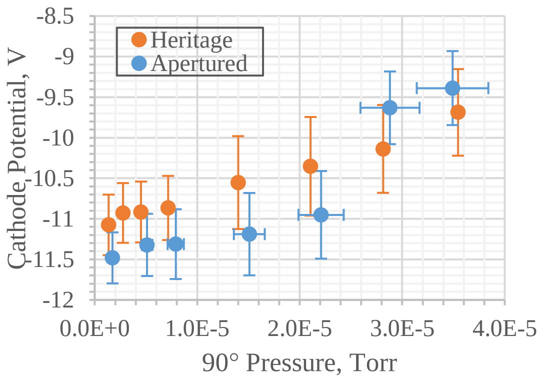

b)

Figure 2. a) Anode current peak fluctuation frequency (filled) and amplitude (open) b) Cathode-to-ground voltage and standard deviation of fluctuations versus background pressure

Figure 2a) tracks the frequency and amplitude of the breathing mode that dominates anode current fluctuations as a function of background pressure and shows a substantial difference in the amplitude of the breathing mode between the two tests. It is unclear what conditions in the heritage probe experiments led to breathing mode amplitude several times smaller than observed in the apertured probe experiments. In both experiments the breathing mode amplitude and frequency are non-monotonic functions of background pressure.

Fast Fourier transforms (FFT's) of the discharge current and cathode potential oscillations are averaged over several hundred measurements and shown for the heritage probe experiments in Fig. 3 and Fig. 4. Only the breathing mode at 10-30 kHz and an unidentified oscillation in the 4-8 MHz range exhibit a strong frequency dependence on background pressure for either the anode current or cathode potential waveforms. The anode current FFT's in Fig. 3a) also show a pressure dependent mode at ~300 kHz which generally decreases in amplitude (except at 10 times baseline pressure) as the pressure rises. The cathode potential oscillations in Fig. 3b) appear to gradually increase in magnitude with pressure across a broad band of frequencies spanning from about 30 kHz to 2 MHz. Power spectra of the cathode potential fluctuations appear similar to the anode current spectra at frequencies below 100 kHz, but higher frequency components become far more pronounced. We do not account for filtering of the high frequency signal components by the stray capacitance of the measurement circuit here, but it is likely that a calibrated result will show oscillations in the 1-10 MHz band being of the same order or larger than the breathing mode contribution to cathode potential fluctuations.

Figure 5 tracks the frequency (solid markers) and magnitude (open markers) of the 4-8 MHz peak in the two power spectra (anode current and cathode potential) as a function of background pressure. There is a starkly linear dependence of the frequency on background pressure for both anode current and cathode potential fluctuations. Both power spectra have magnitudes that peak at around 10-15 times the baseline pressure. The cathode potential spectra show a large jump in magnitude of the 4-8 MHz mode going from 5 to 10 times baseline pressure that appears to be related to an overlap with a smaller peak at a roughly pressure independent frequency of ~5.5 MHz visible in Fig. 4. The 5.5 MHz mode may be involved in wave coupling interactions between the pressure dependent mode at 4-8 MHz and the pressure-independent fluctuations that peak near 2 MHz.

The 4-8 MHz mode is similar in frequency range to azimuthally propagating waves that have been measured in a variety of other Hall thrusters and linked with cross-field electron transport[11-14], although the fluctuations observed here are in highly spatially averaged parameters that are unlikely to reflect largely azimuthal oscillations. These instabilities are more likely related to the axially propagating modes measured by Tsikata et al. using a collective scattering diagnostic in the near field of a 5kW Hall thruster[14] and identified as the fast ion beam mode of Grésillon & Doviel[15]. A similar dispersion relation and fluctuation frequency was found for a resistive mode in a hybrid PIC model, where ionization effects were taken into account[16]. If the mode observed here is axially propagating with a phase speed near that of the ion beam (u~20km/s) then the wavelength of the mode varies from ~5 mm at the minimum pressure to ~2.5 mm at the maximum pressure (~25 times baseline). This length scale is on the same order as the acceleration region length.

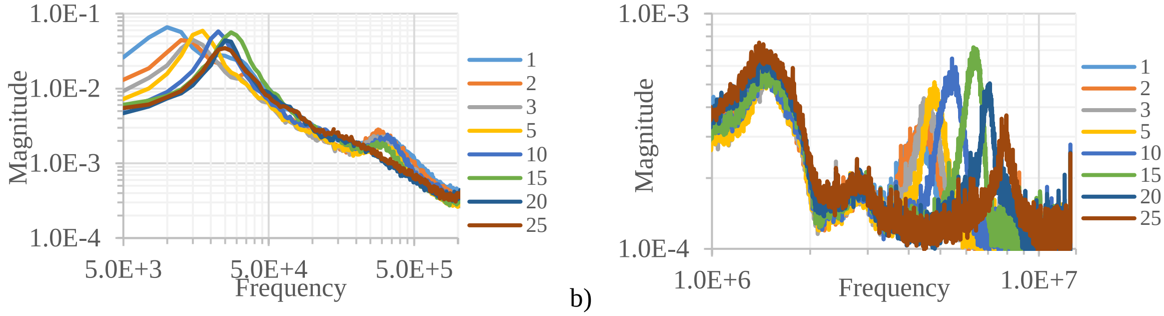

Figure 3. Average power spectral density of anode current waveforms for a range of baseline normalized background pressures shown for a) low frequency and b) high frequency bandwidths.

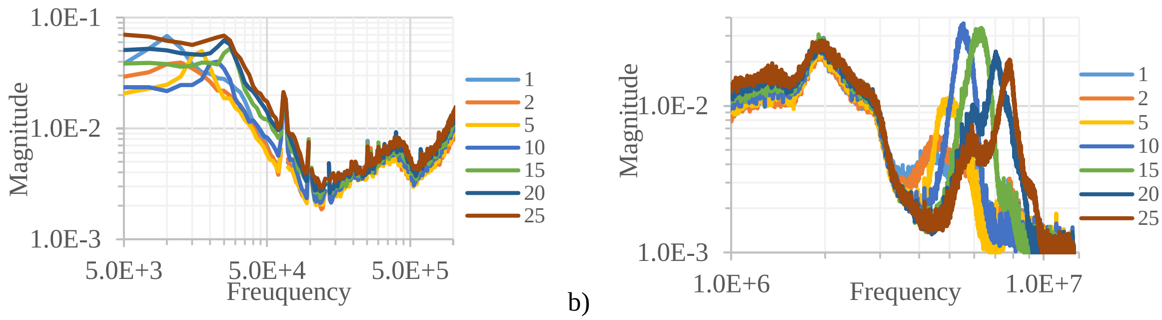

Figure 4. Average power spectral density of cathode-to-ground potential waveforms for a range of baseline normalized background pressures shown for a) low frequency and b) high frequency bandwidths.

A. Neutral Flux Measurements

At each operating pressure the neutral flux probe pressure is recorded as a function of the ion retarding grid voltage for a constant electron repelling voltage (-20V for the heritage probe and -100V for the aperture probe) at three positions. At the 180° position (pointing downstream, adjacent to thruster and 7 cm upstream of the exit) and 90° (pointing radially towards the thruster axis from 43 cm downstream of the exit) position there was no apparent dependence of the pressure on ion retarding grid voltage. At the 30° position (pointing toward thruster from 1 m away, 30° from thruster axis) the neutral flux probe pressure (normalized to its maximum value) is shown in Fig. 3 for the heritage probe as a function of ion retarding voltage (with respect to ground) for different background pressures (normalized to the minimum value) ranging from the baseline pressure of 1.4×10^{-6} Torr to 2.8×10^{-5} Torr (20X). The figure shows the neutral flux probe pressure acting analogous to a retarding potential analyzer, as was shown in a similar neutral flux probe designed and operated by King and Gallimore[10].

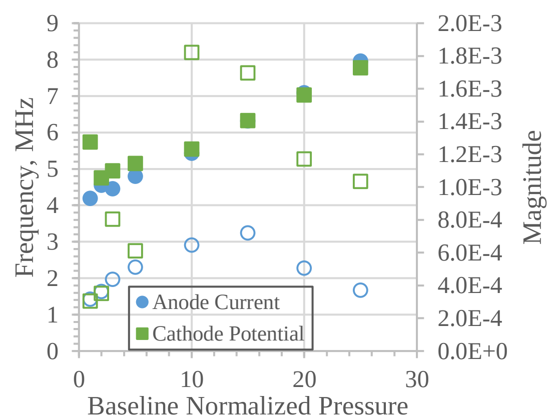

Figure 5. Peak frequency (filled) and magnitude (open) of high frequency anode current (circle) and cathode potential (square) fluctuations as a function of background pressure normalized to baseline.

The ratio of the pressure drop, ΔP, to the ion flux, Γ_i, measured at 30° is shown in Fig. 6 for both neutral flux probe configurations. For the heritage probe tests the ion flux was measured by a 0.50 inch diameter planar Langmuir probe flush with a 0.75 inch diameter ceramic tube. The planar probe was placed on a separate rotation table and rotated into the same 30° location where the ΔP measurements are made while the neutral flux probe is stowed at 180°. The apertured probe allows for the ion flux to be measured by the front aperture plate of the probe itself which is biased to -100 V for the data shown here.

The vertical error bars shown in Fig. 7 reflect the standard deviation of 5 separate measurements of ΔP made with the apertured probe, while the horizontal error bars reflect the assumed uncertainty of the pressure values. The heritage probe data reflect a single measurement at each pressure.

Both configurations show measured values of $\beta \equiv \Delta P/(ST_1\Gamma_i)$ that are always less than unity – the value expected based on Eq. (4) - with a trend of β decreasing as pressure increases for the lowest pressures measured. The two probes measure a fairly constant β between 0.4 and 0.7 at high pressure.

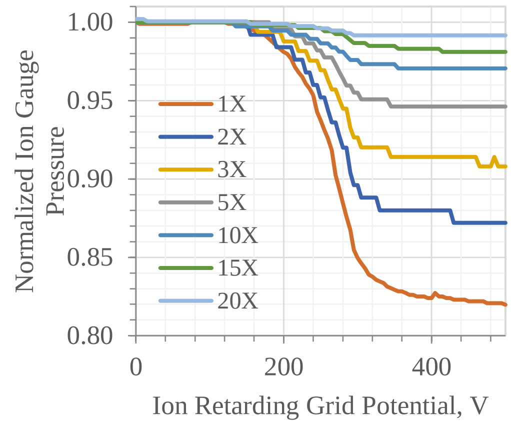

Figure 6. Normalized neutral flux probe pressures as a function of ion retarding grid potential with respect to ground for various values of normalized background pressure for the heritage probe.

It is presently unclear why the two probes measure $\beta < 1$. In the framework of the analysis above, a possible explanation is that the effective Clausing factor for neutrals exiting the ionization gauge to exit the probe assembly is around twice the effective Clausing factor for ions entering the probe assembly to enter the ionization gauge, resulting in $\beta \sim 0.5$. It is also plausible that the effective Clausing factor for ions depends on the retarding potential which can lead to non-unity values of β that depend on the transmission, T_1. In either of these cases the low measured β does not represent a correction factor needed for the predominantly neutral flow measurements made at 90° and 180°.

Alternatively, the low and pressure dependent β values measured may be due to errors in the measurement, such as an inaccurate xenon correction factor, overestimation of the ion flux (e.g. from ion collection area expansion beyond the probe cross section), measurement prior to steady state attainment (i.e. while the pressure is still dropping due to finite conductance) or a contaminated ionization gauge signal. In the case of an inaccurate xenon correction factor we would still expect a constant value of β, though the background pressure may affect the other sources of error. Gradients in the gas temperature are also neglected, which may play a role near the electron repelling grid and the ionization gauge which are expected to be hotter than the rest of the assembly. The analysis neglects particle collisions, reasonably since the highest gauge pressure of 3.5×10^{-5} Torr corresponds to a xenon-xenon collision mean free path of >1 m.

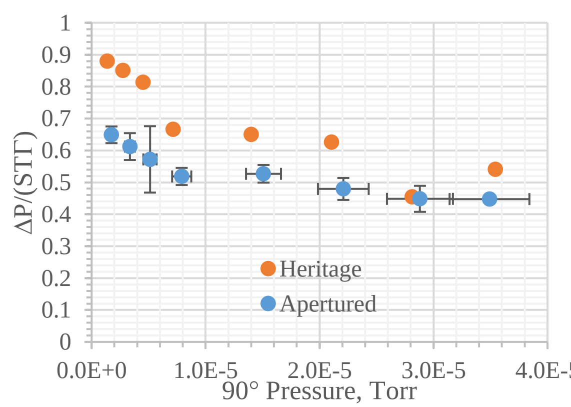

Figure 7. Ratio of the neutral flux probe ΔP to the ion flux, normalized by the grid transparency product with S, as a function of chamber pressure measured by the neutral flux probe in the 90° position for both probe configurations.

We assume the ion beam is fully singly ionized when converting the current densities measured by the planar Langmuir probes into particle densities. This contributes to the underestimation of β, but we expect the combined flux of doubly and triply charged xenon to be less than 20% of the total ion flux and to lead to a β reduction that is also below 20%.

The backstreaming neutral flux at 180° is estimated using Eq. (1) and shown in Fig. 8 as solid lines. Figure 8 also shows the neutral flux estimate divided by the β values from Fig. 4 as dashed lines – this would correspond to a calibrated flux estimate if the Fig. 7 data are interpreted as due to an inaccurate pressure reading (there is no evidence at this time to support this interpretation). The circles in Fig. 8 represent the change in anode mass flow rate required at each elevated background pressure in order to maintain a constant discharge current (i.e. how much lower is the flow than at the lowest background pressure). These mass flow rate changes are converted to neutral xenon flux at the thruster inlet using the approximate discharge channel area of 60 cm^2. The uncertainty of the flow rate is estimated to be about 1%.

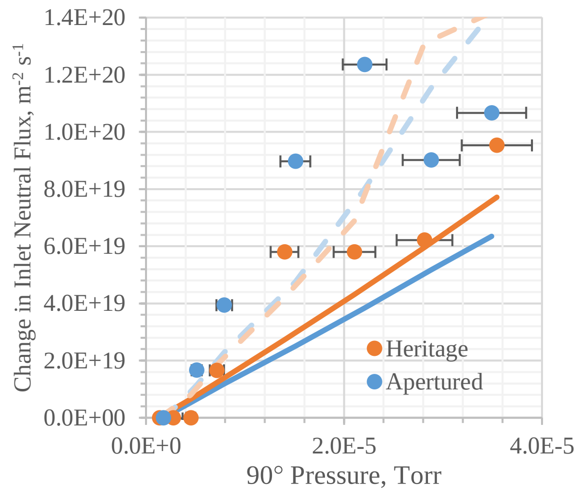

Figure 8. Difference in anode flow rate at baseline pressure and flow rate at various elevated pressures divided by the channel area compared to the neutral flux probe measurements at 180° (solid lines). Neutral flux probe measurements divided by β are shown as dashed lines.

The anode flow rate changes with background pressure shown in Fig. 8 are not balanced by the measured increases in backstreaming neutrals even when one assumes the β values from Fig. 7 as calibration factors, though the two fluxes remain of the same order of magnitude. Experiments performed with the heritage neutral flux probe exhibit an interesting behavior where the anode mass flow rate remains constant from baseline pressure (1.4×10^{-6} Torr) to over 3 times higher (4.5×10^{-6} Torr), followed by a rapid drop in flow rate as the pressure is raised up to 10 times baseline (1.4×10^{-5} Torr) then another levelling off of anode flow from 10 times to 20 times (2.8×10^{-5} Torr) baseline. These stepwise trends are not reflected by the backstreaming neutral flux (or the cathode potential) which increases monotonically.

The two plateaus in anode flow rate (from 1 to 3X and 10 to 20X baseline pressure) may indicate competing trends in opposing directions. For example, increasing pressure may decrease the confinement time of electron which would lead to decreased ionization rates to offset the increase in neutral density and possible increase in recycled electron current. Unfortunately, near field Langmuir probe measurements were not taken at any two pressures on the same plateau to compare shifts in the plasma at these unexpected conditions.

Experiments performed with the apertured probe demonstrate a larger disparity between anode flow rate changes and backstreaming neutral flux measurements. The anode flow rate drops 5.7% below the baseline value (baseline anode flow is 20.82 sccm xenon) at 13 times the baseline pressure (2.2×10^{-5} Torr compared to 1.7×10^{-6} Torr baseline) while the backstreaming flux increases by 1.8% compared to the baseline inlet flux. The apertured experiments also show a counterintuitive increase in anode flow rate necessary as the background pressure was increased from 13 times to 17 times baseline pressure, which may be related to the jump down in cathode-to-ground voltage amplitude seen in Fig. 2b) at these pressures. These trends again indicate a more complicated phenomena at play in anode current pressure dependence beyond the simple ingestion of background neutrals.

B. Near Field Langmuir Probe Measurements

The near field probe diagnostic was continuously translated laterally across the thruster face (x-direction) at a variety of axial (z-direction, measured from pole piece face) and vertical (y-direction) probe stage positions creating 3-dimensional maps of plasma parameters in the near field at the baseline pressure condition. Here we focus on pressure dependencies of parameter maps taken in the x-z plane at the height of the thruster axis (i.e. y=0 for a thruster axis-oriented coordinate system). A description of the data analysis techniques is given in the appendix.

Figure 9 picks out three of the main plasma parameters (electron density, plasma potential and axial ion current density) and plots them at four different pressures: baseline or 1X (1.4×10^{-6} Torr), 5X (2.8×10^{-6} Torr), 15X (2.1×10^{-5} Torr), and 25X (3.5×10^{-5} Torr). The inner discharge channel wall is located near ±25 mm and the outer wall is near ±50 mm for reference.

Several trends are clear from Fig. 9 including the well documented observation of an upstream shifting potential structure as the background pressure is increased[5,6]. The plasma potential drops from roughly 50V near the discharge channel at baseline pressure to under 30V at 25X with a similar size decrement in plasma potential near the thruster axis. The electron density appears to increase as in the near plume as the background pressure rises, particularly on-axis and 75 mm downstream at the discharge channel outer radius. The density decreases with increased pressure in the periphery of the beam, i.e. near the exit at radial locations greater than the outer radius of the channel or smaller than the inner radius of the channel.

The axial ion current density, which is linearly extrapolated to estimate the value at the floating potential, exhibits changes in topology that appear consistent with the upstream shift in the plasma as pressure is increased. The decrease in axial flux at high angles from the channel is expected to be a by-product of greater ion loss to the channel walls for the upstream shifted plasma. We also observe a 'forking' of the on-axis ion flux at higher pressure which may also be related to the collimation of the ion beam by the channel walls.

IV.Conclusion

Experiments were performed that add to the open literature on background pressure effects on Hall thruster operation. Notable observations include the appearance of a 4-8 MHz fluctuation in anode current and cathode voltage with a linear scaling of frequency with background pressure. This is expected to be an ion mode, but the source of the instability and reason for its pressure scaling require further study.

Unexpected trends were observed in the anode mass flow required to maintain a constant discharge current under various background pressures. In one configuration, the anode flow remained constant despite a tripling of the background pressure, rose rapidly from 5 to 10 times baseline pressure, then remained constant again across a further doubling of the pressure. In the second configuration the anode flow dropped steadily with pressure up until 17 times baseline pressure where the anode flow rate suddenly rose, the cathode began floating substantially closer to ground, and the thruster body current tripled from 40mA to 120mA. This transition also led to the disappearance of an anode current oscillation mode in the 200-400 kHz range observed at lower pressures, a change from a growing cathode potential oscillation at 100 kHz to diminishing, and a sudden lack of breathing mode harmonics in the anode current FFT spectrum. These trends suggest a complex competition between mechanisms that increase the anode current with pressure (e.g. increased electron conductivity, near field neutral density and multiply charged ions) and those that reduce anode current (e.g. reduced electron energy, increased wall losses).

An attempt was made to perform an *in situ* calibration of a pair of neutral flux probes (based on an ionization gauge and accommodation volume) using the ion beam of the Hall thruster. The measurements revealed flux values nearly half of those expected based on ion flux data and a variety of possible explanations for this discrepancy were discussed. Improved accuracy is expected if the gauge is positioned closer to the thruster when exposed to the ion beam so the signal is dominated by ion flux, and if care is taken to characterize the gauge settling time when sweeping the ion retarding voltage. Ultimately, a secondary measurement technique is likely necessary to validate the neutral flow measurements.

A concurrent spatial mapping of the near field plasma plume properties was performed using a planar Langmuir probe. These maps reveal an upstream shift in the ion acceleration as has been observed in other Hall thrusters with optical diagnostics. An important trend is the reduction in the electric field strength throughout the near-field region as pressure is increased. This may be expected to follow from the increase in the proportion of slow ions (through charge exchange and possibly external ionization) making up the beam. Slow ions stream readily to lower potentials, reducing gradients in the highly peaked potential and density profiles. Reduced electric field strengths reduces the electrostatic confinement of electrons along magnetic field lines which may allow increased mobility in the near plume if electrons can stream to regions of low magnetic field strength to be scattered classically. Enhanced off-axis ion fluxes may also make it easier for an off-axis cathode to neutralize the beam as less cross-magnetic field transport is required, reducing the cathode-to-ground voltage.

Much work remains in characterizing the near-field plume properties that lead to the observed changes in thruster operation with background pressure. If cross-field electron mobility is a strong function of the background pressure, the source of the mobility still needs to be demonstrated empirically. A kinetic model of electron dynamics in the near field is suggested as a key towards disambiguating the main factors that allow the cathode electrons to neutralize the beam and couple to the thruster while maintaining an equipotential, net current-free boundary condition in the vacuum chamber.

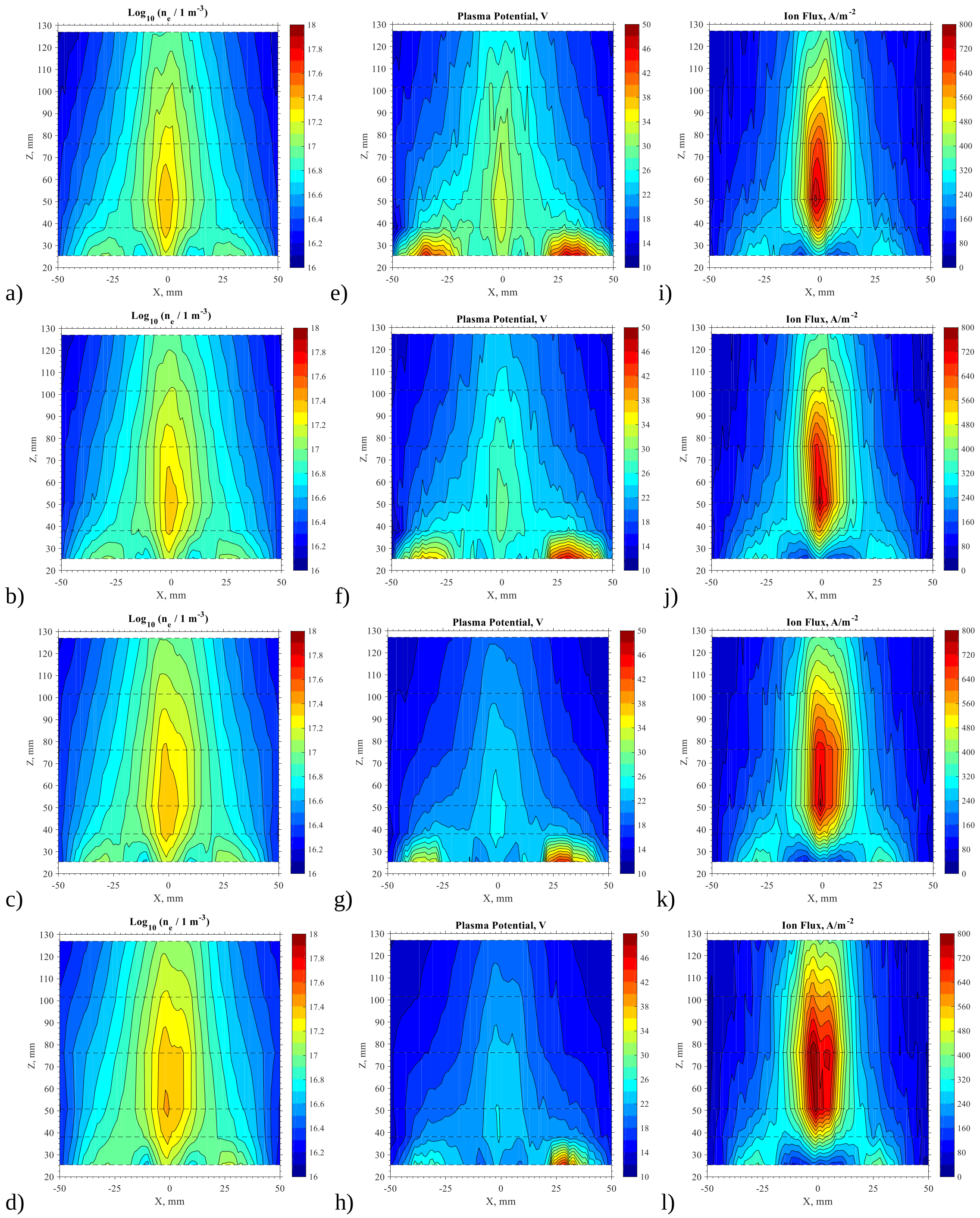

Figure 9. Plasma parameter contours in the near field plume at different background pressures from left to right a) log10 of plasma density at 1X, b) 5X, c) 15X, and d) 25X pressures, e)-h) show plasma potential with respect to ground at the 1X, 5X, 15X and 25X pressures respectively, and i)-l) show the ion flux at the 1X, 5X, 15X and 25X pressures. Dashed lines show axial distances where measurements were taken.

Appendix

The 1-sided planar probe analysis is taken largely from the derivation presented by Woods & Sudit[17] where it is shown that the derivative of the collected electron current with respect to the sheath voltage, $V_{sh}=V_s-V$, is proportional to the 1-sided electron velocity distribution function (EVDF) projected along the probe normal (here V_s denotes the sheath edge/plasma potential and V the probe potential) i.e.

$$\frac{dI}{dV} = \frac{A_p e^2}{m_e} H\left(\sqrt{\frac{2eV_{sh}}{m_e}}\right) \tag{A1}$$

Here H is the z-projected EVDF defined as,

$$H(v_z) = \int_{-\infty}^{\infty}\int_{-\infty}^{\infty} f(v_x, v_y, v_z)\, dv_y\, dv_x \tag{A2}$$

We can see from the first equation that the slope reaches a maximum when the probe is biased to the plasma potential, i.e. $V=Vs$, as long as there is not a majority population of electrons with a large drift component in the z direction (probe normal). The plasma potentials reported here are taken as the potential where dI/dV is a maximum. We take the electron current as raw probe current, since any slope due to the ion current is negligible in comparison.

Once we know the plasma potential we can use H from the above equation to find moments of the 1-D EVDF such as density, n_e, and average kinetic energy, E_e, which we have defined here to be equivalent to electron temperature for a drift-free population:

$$n_e = \int_{-\infty}^{\infty} H(v_z) dv_z \tag{A3}$$

$$E_e = \langle m v_z^2 \rangle = \frac{1}{n_e}\int_{-\infty}^{\infty} m v_z^2 H(v_z) dv_z \tag{A4}$$

We note the probe faces only one direction so we must assume a distribution for electrons in the other direction in order to obtain moments of the distribution such as density and temperature (average random kinetic energy). Here we are assuming a symmetric distribution.

Acknowledgments

Contributors to this project included Phil Mak and Jason Young of The Aerospace Corporation. This project was supported by the Independent Research and Development Program at The Aerospace Corporation.

References

[1]Byers, D., and Dankanich, J.W., "A Review of Facility Effects on Hall Effect Thrusters," *IEPC 2009-076*.

[2]Diamant, K., Spektor, R., Beiting, E.J., Young, J.A., and Curtiss, T.J., "The Effects of Background Pressure on Hall Thruster Operation", *AIAA Meeting Paper AIAA-2012-3735*, Atlanta, GA, 2012.

[3]Diamant, K., Lee, T., Liang, R., Noland, J., Vial, V., Cornu, N. "Performance and Plume Characterization of the PPS®1350-G Hall Thruster", *AIAA Meeting Paper AIAA-2016-4543*, Salt Lake City, UT, 2016.

[4]Diamant, K., Liang, R., and Corey, R.L., "The Effect of Background Pressure on SPT-100 Hall Thruster Performance," *AIAA Meeting Paper AIAA-2014-3710*, Cleveland, OH, 2014.

[4]Hofer, R.R., and Anderson, J.R., Finite Pressure Effects in Magnetically Shielded Hall Thrusters," *AIAA Meeting Paper AIAA-2014-3709*, Cleveland, OH, 2014.

[5]Nakles, M.R., and Hargus, W.A., Jr., "Background Pressure Effects on Ion Velocity Distribution Within a Medium-Power Hall Thruster," *Journal of Propulsion & Power*, Vol. 27, No. 4, Jul-Aug 2011, pp. 737,743.

[6]Spektor, R., Tighe, W.G., and Kamhawi, H., "Laser Induced Fluorescence Measurements in a Hall Thruster Plume as a Function of Background Pressure", *AIAA Meeting Paper AIAA-2016-4624*, Salt Lake City, UT, 2016.

[7]Randolph, T., Kim, V., Kaufman, H., Kozubsky, K., Zhurin, V., and Day, M., “Facility Effects on Stationary Plasma Thruster Testing”, *IEPC 1993-93*.

[8]Frieman, J.D., Liu, T.M., and Walker, M.L.R., “Background Flow Model of Hall Thruster Neutral Ingestion”, *Journal of Propulsion and Power*, Vol. 33, No. 5, Jan. 2017, pp.1087, 1101.

[9]Raitses, Y., Dorf, L.A., Litvak, A.A., and Fisch, N.J., “Plume Reduction in Segmented Electrode Hall Thruster”, *Journal of Applied Physics*, Vol. 88, No. 3, Aug. 2000, pp.1263, 1270.

[10]King, L.B., and Gallimore, A. D., “Gridded Retarding Pressure Sensor for Ion and Neutral Particle Analysis in Flowing Plasmas,” *Rev. Sci. Instrum.*, Vol. 68, No. 2, Feb. 1996, pp. 1183, 1188.

[11]Litvak, A.A., Raitses, Y., and Fisch, N.J., “Experimental Studies of High-Frequency Azimuthal Waves in Hall Thrusters,” *Physics of Plasmas*, Vol. 11, No. 4, Apr. 2005, pp. 1701, 1705.

[12]Lazurenko, A., Krasnoselskikh, V., and Boucoule, A., “Experimental Insights Into High-Frequency Instabilities and Related Anomalous Electron Transport in Hall Thrusters,” *IEEE Trans. On Plasma Sci.*, Vol. 36, No. 5, Oct. 2008, pp. 1977, 1988.

[13]Cavalier, J., Lemoine, N., Bohomme, G., Tsikata, S., Honoré, C., and Grésillon, D., “Hall Thruster Plasma Fluctuations Indentified as the ExB Electron Drift Instability: Modeling and Fitting on Experimental Data,” *Physics of Plasmas*, Vol. 20, 082107, 2003, pp. 1,11.

[14]Tsikata, S., Lemoine, N., Pisarev, V., and Grésillon, D., “Dispersion Relations of Electron Density Fluctuations in a Hall Thruster Plasma, Observed by Collective Light Scattering,” *Physics of Plasmas*, Vol. 16, 033506, 2009, pp. 1,10.

[15]Grésillon, D., and Doveil, F., “Normal Modes in the Ion-Beam-Plasma System,” *Physical Review Letters*, Vol. 34, No. 2, Jan. 1975, pp. 77,80.

[16]Fernandez, E., Scharfe, M.K., Thomas, C.A., Gascon, N., and Cappelli, M.A., “Growth of Resistive Instabilities in ExB Plasma Discharge Simulations,” *Physics of Plasmas*, Vol. 15, 012102, 2008, pp. 1,10.

[17]Woods, R.C., and Sudit, I.D., “Theory of Electron Retardation by Langmuir Probes in Anisotropic Plasmas,” *Physical Review E*, Vol. 50, No. 3, Sep 1994, pp. 2222,2238.